

Torsion Graph Neural Networks

Cong Shen, Xiang Liu, Jiawei Luo and Kelin Xia

Abstract—Geometric deep learning (GDL) models have demonstrated a great potential for the analysis of non-Euclidian data. They are developed to incorporate the geometric and topological information of non-Euclidian data into the end-to-end deep learning architectures. Motivated by the recent success of discrete Ricci curvature in graph neural network (GNNs), we propose TorGNN, an analytic Torsion enhanced Graph Neural Network model. The essential idea is to characterize graph local structures with an analytic torsion based weight formula. Mathematically, analytic torsion is a topological invariant that can distinguish spaces which are homotopy equivalent but not homeomorphic. In our TorGNN, for each edge, a corresponding local simplicial complex is identified, then the analytic torsion (for this local simplicial complex) is calculated, and further used as a weight (for this edge) in message-passing process. Our TorGNN model is validated on link prediction tasks from sixteen different types of networks and node classification tasks from three types of networks. It has been found that our TorGNN can achieve superior performance on both tasks, and outperform various state-of-the-art models. This demonstrates that analytic torsion is a highly efficient topological invariant in the characterization of graph structures and can significantly boost the performance of GNNs.

Index Terms—Geometric deep learning, Graph neural networks, Analytic torsion, Message Passing.



1 INTRODUCTION

WITH the accumulation of non-Euclidean data, the development of deep learning models, which have revolutionized sequence and image data analysis [1], has given rise to geometric deep learning (GDL). Among all the non-Euclidean data are graphs and networks, which are arguable the most powerful topological representation of real-world data and systems. As a special type of GDL, graph neural networks (GNNs) have demonstrated remarkable learning capability and have become prevalent models for various graph tasks, such as node classification, link prediction, and graph classification [2], [3], [4], [5]. GNNs have achieved great success in applications, such as molecule property prediction [6], recommender systems [7], natural language processing [8], critical data classification [9], computer vision [10], particle physics [11], and resource allocation in computer networks [12]. Recent years have seen a rapid increase of research in the field of GNNs. Great efforts have been devoted to algorithm efficiency improvement (especially for large graphs), special architecture design, and various applications [13].

In general, GNN models can be divided into several types, including recurrent-based GNNs, convolution-based GNNs, graph autoencoders, graph reinforcement learning, and graph adversarial networks [13], [14]. The recurrent-based GNNs refer to the initial GNN models, which employ recurrent units as its combination functions. Typical examples

are CommNet [15] and GG-NN [16]. The convolution-based GNNs expand the idea of convolution in the graph space to graph spectral space, based on spectral graph theory. These models are computationally much more affordable, flexible, and scalable. Examples of these models include GCN [2], CurvGN [17], FastGCN [18], Cluster-GCN [19], LGCL [20], ST-GCN [21], AGCN [22] and SGCs [23]. Graph Autoencoder (GAE) is a different type of GNNs, which converts the graph structure into a latent representation (i.e., encoding), that can be later expanded to a graph structure as close as possible to the original one (i.e., decoding). NetRA [24] is a classical GAE with a good performance. Finally, graph reinforcement learning and graph adversarial networks are newly-proposed GNNs that combine reinforcement learning and generative confrontation networks with graph neural architecture. Typical models include MolGAN [25] and MINERVA [26]. In terms of application, recurrent-based GNNs are mainly used in sequence data; Convolution-based GNNs are mainly used in various graphs, networks or knowledge graphs; Graph autoencoders are mainly used in the field of unsupervised models, which are suitable for feature selection or dimensionality reduction; Graph reinforcement learning and graph adversarial networks are applied to generative models, such as molecular generation.

Even with the great development and progress in GNNs, the incorporation of geometric and topological information into graph neural architecture is still a key issue for all GNN and GDL models. Recently, discrete Ricci curvatures have been used in the characterization of “over-squashing” phenomenon [27], which happens at the bottleneck region of a network where the messages in GNN models propagated from distant nodes distort significantly. Curvature-based GNNs have been developed by the incorporation of Ollivier Ricci curvature, a discrete Ricci curvature model, into GNN models and have achieved great success in various synthetic and real-world graphs, from social networks, coauthor networks, citation networks, and Amazon co-purchase graphs [17], [28]. The model can significantly outperform state-of-

- Cong Shen and Jiawei Luo are with College of Computer Science and Electronic Engineering, Hunan University, Changsha, China, 410000. E-mail: {cshen,luojiawei}@hnu.edu.cn. Cong Shen is also with School of Physical and Mathematical Sciences, Nanyang Technological University, Singapore, 637371.
- Xiang Liu is with Chern Institute of Mathematics and LPMC, Nankai University, Tianjin, China, 300071. E-mail: liuxiangmath@163.com. Xiang Liu is also with School of Physical and Mathematical Sciences, Nanyang Technological University, Singapore, 637371.
- Kelin Xia is with School of Physical and Mathematical Sciences, Nanyang Technological University, Singapore, 637371. E-mail: xiakelin@ntu.edu.sg

Corresponding author: Jiawei Luo and Kelin Xia

Manuscript received April 19, 2005; revised August 26, 2015.

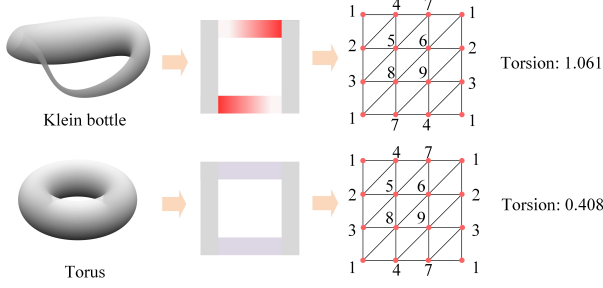


Fig. 1. **The illustration of characterization capability of analytic torsion for Klein bottle and torus surface.** Both Klein bottle and torus surface can be obtained by “gluing” together their edges. A twist exists in Klein bottle when its upper-side is “glued” with low-side as indicated by red colors, i.e., regions in upper edge and low edge are glued together when they are of the same color. More specifically, the two manifolds can be discretized into two simplicial complexes with vertices of same numbers gluing together. Using 1D Hodge Laplacians, analytic torsion for Klein bottle and torus are 1.061 and 0.408, respectively.

the-art models when the underlying graphs are of large-sized and dense [17], [28].

Analytic torsion, which is an alternating product of determinants of Hodge Laplacians, is a topological invariant which can distinguish spaces that are homotopy equivalent but not homeomorphic [29], [30]. Analytic torsion is introduced as the analytic version of Reidemeister torsion (or R-torsion for short), which is an algebraic topology invariant that takes values in the multiplicative group of the units of a commutative ring [31]. R-torsion was developed for the classification of three dimensional (3D) lens spaces in 1935 by Reidemeister [32]. It is found that a complete classification of 3D lens spaces can be achieved in terms of R-torsion and fundamental group [29]. To describe the R-torsion in analytic terms, Ray and Singer defined the analytic torsion for any compact oriented manifold and orthogonal representation of the fundamental group [31]. Their definition uses the spectrum of the Hodge Laplacian on twisted forms. When the orthogonal representation is acyclic and orthogonal, Cheeger and Müller proves that the R-torsion is equivalent to analytic torsion [33], [34]. With the unique characterization capability, analytic torsion provides a powerful representation of the topological and geometric information within the data. As demonstrated in Figure 1, both Klein bottle and torus surface can be obtained by “gluing” together the upper edge with lower one and left edge with right one. However, a twist exists in Klein bottle when its upper-side is glued with low-side as indicated by red colors, i.e., regions in upper edge and low edge are glued together when they are of the same color. This can be seen more clearly if the manifolds are discretized into two simplicial complexes with vertices of same numbers gluing together. Interestingly, the topological difference between Klein bottle and torus surface can be well characterized by their analytic torsion. The unique characterization capability of analytic torsion makes it an efficient topological invariant for GNNs, and more general GDLs.

Here we propose a new graph neural network model called analytic Torsion enhanced Graph Neural Network (TorGNN). An analytic torsion based message passing pro-

cess is developed in our TorGNN. Mathematically, a local simplicial complex is constructed for each edge, and its analytic torsion is used as the weight of the special edge in node feature aggregation. Our TorGNN model shows the best performance and outperforms all state-of-the-art methods, on link prediction tasks from 16 different datasets and node classification tasks from 3 different datasets. This demonstrate that our TorGNN can better capture the complexity of the local structure of graph data.

2 RELATED WORK

2.1 Geometry-aware graph neural networks

Geometry-aware GNNs have been proposed to incorporate algebraic and geometric information of graph data, though the refined message passing and aggregation mechanisms. Among them is TFN, which is a SE(3) equivariant GNN model based on the group set of 3D translation and rotation transformations [35]. LieConv is based on Lie group set of differential transformations beyond 3D translations and rotations [36]. EGNN makes use of all n -dimension Euclidean transformations including translations, rotations and reflections [37].

In addition, other GNN models take into account the curvature information, such as CurvGN [17], SELFMSGNN [38] and CurvGAN [28]. CurvGN is the first graph convolutional network built on advanced graph curvature information. SELFMSGNN is the first attempt to study the self-supervised graph representation learning in the mixed-curvature spaces. CurvGAN is the first GAN-based graph representation method in the Riemannian geometric manifold. Curvature has also been combined with hyperbolic graph neural networks, such as, HGCN [39], HAT [40], HGNN [41], ACE-HGNN [42] and HRGCN+ [43].

2.2 Analytic Torsion

The Reidemeister torsion, or R-torsion, was proposed by Kurt Reidemeister in 1935 [32]. It is the first topological invariant that could distinguish spaces with the same homotopy type. With fundamental group, it has been used in the complete classification of 3D lens spaces. In 1970s, Ray and Singer introduced the analytic torsion as the analytic version of Reidemeister torsion for any compact oriented manifold and orthogonal representation of the fundamental group [31]. When the orthogonal representation is acyclic and orthogonal, Cheeger and Müller proves that the R-torsion is equivalent to analytic torsion [33], [34]. Computationally, analytic torsion can be calculated from the determinants of Hodge Laplacians [30]. Note that for Hodge Laplacians with zero eigenvalues, the determinant is replaced by the multiplication of all non-zero eigenvalues. With the unique characterization capability, analytic torsion provides a powerful representation of the topological and geometric information within the data. As far as we know, this is the first attempt to combine analytic torsion and GNNs.

3 TORGNN

3.1 Notations and Problem Formulation

Notations Let $G = (V, E)$ represents a graph with nodes $v_i \in V$ (x and y are also used to denote nodes) and

edges $(v_i, v_j) \in E$. Node features are denoted as $H = \{h_1, \dots, h_N\} \in \mathbb{R}^{N \times m}$. A total number of N nodes in vertex set V and each node is encoded with a predefined m -dimension attribute vector (e.g., a generated graph embedding or a one-hot coding). We use $\mathcal{N}(x)$ to denote the neighbors of node x , $d(x)$ represent node degree of nodes x .

We use K to represent a simplicial complex, $K_{x,y}$ the local simplicial complex from nodes x and y , and $T(K_{x,y})$ the analytic torsion for local simplicial complex $K_{x,y}$. The p -th Hodge Laplacian is denoted as L_p and its determinant is denoted as $|L_p|$. If the matrix has zero eigenvalues, the determinant $|L_p|$ equals to the multiplication of all non-zero eigenvalues. The p -th boundary matrix is denoted as B_p . Zeta function can be defined based on the eigenvalues of L_p and is denoted as $\zeta_p(s)$.

Problem formulation We consider two types of tasks, one is link prediction and the other is node classification. The link prediction task is to learn a mapping function $\Phi : E \rightarrow [0, 1]$ from edges to scores, such that we can obtain the probability of two arbitrary nodes interacting with each other. Similarity, node classification is to learn a mapping function $\Psi : V \rightarrow \mathbb{R}_c^N$ from nodes to vectors and N_c is dimension of node's labels.

3.2 Analytic torsion

3.2.1 Simplicial complex

As a generalization of graph, a simplicial complex K is composed of simplices. A simplex with $p + 1$ vertices from a vertex set V is called a p -simplex, denoted by $\sigma^p = \{v_0, v_1, \dots, v_p\}$. For a p -simplex σ^p , any nonempty subset is called its face. A face of σ^p with $p - 1$ dimension is called a boundary of σ^p . Geometrically, a p -simplex can be seen as the convex hull formed by $p + 1$ affinely independent points. In this way, 0-simplex is a vertex, 1-simplex is an edge, 2-simplex is a triangle, and 3-simplex is a tetrahedron.

3.2.2 Combinatorial Laplacian of simplicial complex

Given an oriented simplicial complex K , that is, a simplicial complex with an order on the vertex set, we use $Z/2$ coefficient and denote a p -simplex as $\sigma^p = [v_0, v_1, \dots, v_p]$. A p -chain is defined as a finite sum of p -simplices in K , denoted as $c = \sum_i \sigma_i^p$. Let C_p be the set of p -chains of K , which is spanned by p -simplices of K over $Z/2$, called the p -chain group of K . The boundary operator $\partial_p : C_p \rightarrow C_{p-1}$ for a p -simplex σ^p is defined as follows,

$$\partial_p \sigma^p = \sum_{i=0}^p (-1)^i [v_0, \dots, \hat{v}_i, \dots, v_p]$$

where \hat{v}_i means that v_i has been removed. The boundary operator satisfies $\partial_{p-1} \partial_p = 0$. These chain groups together with boundary operators form a chain complex,

$$0 \xleftarrow{\partial_0} C_0 \xleftarrow{\partial_1} \dots \xleftarrow{\partial_p} C_p \xleftarrow{\partial_{p+1}} \dots$$

Considering the canonical inner product on chain groups, that is, let all the simplices orthogonal. Denote the adjoint of ∂_p by δ^p , then the p -th Hodge (combinatorial) Laplacian operator of K is defined as,

$$\Delta_p = \delta^p \partial_p + \partial_{p+1} \delta^{p+1}.$$

Let B_p be the matrix form of ∂_p , then, the p -th Hodge Laplacian matrix of K is,

$$L_p = B_p^T B_p + B_{p+1} B_{p+1}^T. \quad (1)$$

For 1-dimension simplicial complex K , i.e., a graph, we have $L_0 = B_1 B_1^T$, which is the graph Laplacian. Further, for an n -dimension simplicial complex K , its highest order Hodge Laplacian is $L_n = B_n^T B_n$.

The Hodge Laplacian matrices in Eq.(1) can be explicitly described in terms of simplex relations. More specifically, L_0 can be expressed as,

$$L_0(i, j) = \begin{cases} d(\sigma_i^0), & \text{if } i = j \\ -1, & \text{if } i \neq j \text{ and } \sigma_i^0 \cap \sigma_j^0 \\ 0, & \text{if } i \neq j \text{ and } \sigma_i^0 \not\cap \sigma_j^0 \end{cases}$$

where $d(\sigma_i^0)$ is the degree of vertex σ_i^0 . Furthermore, when $p > 0$, L_p can be expressed as

$$L_p(i, j) = \begin{cases} d(\sigma_i^p) + p + 1, & \text{if } i = j \\ 1, & \text{if } i \neq j, \sigma_i^p \not\cap \sigma_j^p, \sigma_i^p \cup \sigma_j^p \text{ and } \sigma_i^p \sim \sigma_j^p \\ -1, & \text{if } i \neq j, \sigma_i^p \not\cap \sigma_j^p, \sigma_i^p \cup \sigma_j^p \text{ and } \sigma_i^p \approx \sigma_j^p \\ 0, & \text{if } i \neq j, \sigma_i^p \cap \sigma_j^p \text{ or } \sigma_i^p \not\cup \sigma_j^p \end{cases}$$

here $d(\sigma_i^p)$ is (upper) degree of p -simplex σ_i^p . It is the number of $(p + 1)$ -simplexes, of which σ_i^p is a face. Notation $\sigma_i^p \cap \sigma_j^p$ represents that two simplexes are upper adjacent, i.e. they are faces of a common $(p + 1)$ -simplex, and $\sigma_i^p \not\cap \sigma_j^p$ represents the opposite. Notation $\sigma_i^p \cup \sigma_j^p$ represents that two simplexes are lower adjacent, i.e. they share a common $(p - 1)$ -simplex as their face, and $\sigma_i^p \not\cup \sigma_j^p$ represents the opposite. Notation $\sigma_i^p \sim \sigma_j^p$ represents that two simplexes have the same orientation, i.e. oriented similarly, and $\sigma_i^p \approx \sigma_j^p$ represents the opposite. The eigenvalues of combinatorial Laplacian matrices are independent of the choice of the orientation.

The Laplacian matrix has various important properties. First, it is always positive semi-definite, thus all its eigenvalues are non-negative. Second, the multiplicity of zero eigenvalues, i.e., the total number of zero eigenvalues, of L_p is equal to the p -th Betti number β_p . In particular, If K is a graph, the number (multiplicity) of zero eigenvalues is equal to the topological invariant β_0 , which counts the number of connected components in the graph. Third, the second smallest eigenvalue, i.e., the first non-zero eigenvalue, is called Fiedler value or algebraic connectivity, which describes the general connectivity. The corresponding eigenvector can be used in classification and clustering.

3.2.3 Analytic torsion for simplicial complex

For an n -dimension simplicial complex K , its p -th Laplacian matrix is $L_p = B_p^T B_p + B_{p+1} B_{p+1}^T$ where B_p is the boundary matrix. Since L_p is a positive semi-definite, all of its eigenvalues, denoted as $\{\lambda_i\}$, are non-negative. A special Zeta function can be defined based on the eigenvalues of L_p as follows,

$$\zeta_p(s) = \sum_{\lambda_i > 0} \frac{1}{\lambda_i^s}.$$

Note that the Zeta function is composed of all the positive eigenvalues L_p .

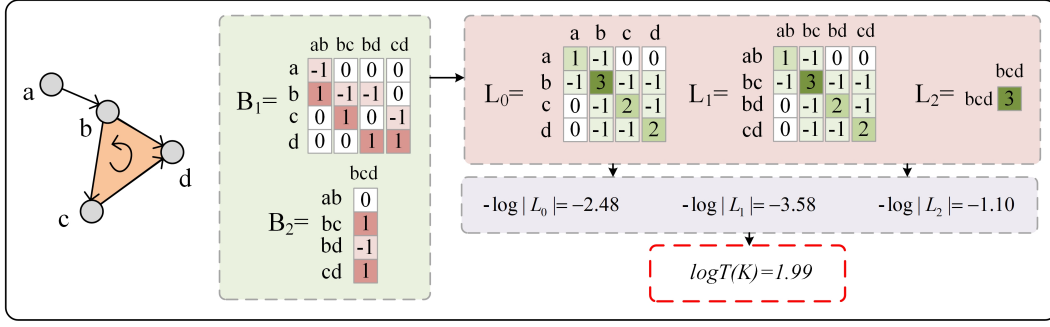


Fig. 2. An example of calculating the logarithm of analytic torsion for a two dimension simplicial complex. Based on the simplicial complex K , we can construct boundary matrices, namely B_1 and B_2 . The Hodge Laplacian matrices, including L_0 , L_1 and L_2 , can be calculated according to Eq. (1). Then, the determinant of Hodge Laplacian matrices $|L_p|$ can be evaluated. Finally, the logarithm of the analytic torsion $\log T(K)$ can be calculated.

The logarithm of analytic torsion $T(K)$ of K can be defined as,

$$\log T(K) = \frac{1}{2} \sum_{p=0}^n (-1)^p p \zeta'_p(0) \quad (2)$$

where $\zeta'_p(0) = \zeta'_p(s=0)$ is the derivative of the Zeta function at $s=0$. Mathematically, if we let $|L_p| = \prod_{\lambda_i > 0} \lambda_i$ be the product of all non-zero eigenvalues of L_p , we have $\zeta'_p(0) = -\log |L_p|$. Further, the logarithm of analytic torsion $T(K)$ can be rewritten as,

$$\log T(K) = \frac{1}{2} \sum_{p=0}^n (-1)^{p+1} p \log |L_p|.$$

Note that the sum is from 0 to n , the highest order of simplicial complex K .

For an 1-dimension simplicial complex K , i.e., a graph, its analytic torsion $T(K)$ can be expressed as,

$$T(K) = |L_1|^{\frac{1}{2}}.$$

Note that here $L_1 = B_1^T B_1$ from Eq.(1). Further, for a 2-dimension simplicial complex K , its analytic torsion $T(K)$ is,

$$T(K) = \frac{|L_1|^{\frac{1}{2}}}{|L_2|^{\frac{1}{2}}}.$$

The analytic torsion is highly related to the dimension of the simplicial complex. Figure 2 illustrates the process to calculate the logarithm of analytic torsion for a 2-dimension simplicial complex.

3.3 Analytic torsion based graph neural networks

In our TorGNN model, the analytic torsion is incorporated into graph neural network architecture by adding analytic torsion into message-passing process.

Analytic torsion based message-passing process: An essential idea of our TorGNN is to aggregate node features by a analytic torsion-based edge weight as follows,

$$h_x^l = \sigma \left(\sum_{y \in \mathcal{N}(x) \cup \{x\}} \frac{1}{\sqrt{d(x)}\sqrt{d(y)}} |\log T(K_{x,y})| W_{\text{GNN}} h_y^{l-1} \right),$$

where $\mathcal{N}(x)$ is the neighbors of node x , $d(x)$ and $d(y)$ represent node degree of nodes x and y respectively, h_x^l

and h_y^{l-1} are the node features of x and y after l and $l-1$ (message-passing) iterations respectively, and W_{GNN} is the weight matrix to be learned.

More importantly, $K_{x,y}$ is the local simplicial complex constructed based on edge x, y . There are various ways to define this local simplicial complex. The most straightforward approach is to build a subgraph using the first-order neighbors. This subgraph contains vertices x, y , and all their neighbors together with all the edges among these vertices. If we allow each triangle in the subgraph to form a 2-simplex, a 2-dimension $K_{x,y}$ can be obtained. Further, we can consider not only the direct neighbors of vertices x and y , but also the indirect neighbors that within l_{sub} steps. An p -simplex ($p \leq n$) is formed among $p+1$ vertices if each two of them form an edge. In general, our local simplicial complex $K_{x,y}$ depends on two parameters, i.e., step l_{sub} for neighbors and simplicial complex order n . The corresponding TorGNN model is denoted as TorGNN(l_{sub}, n).

Our analytic torsion based message-passing process is illustrated in Figure 3. We consider TorGNN(1,1) model, that is the local simplicial complex is constructed using $l_{\text{sub}} = 1$ and $n = 1$. The logarithm of the analytic torsion for the local simplicial complex is used as a weight parameter in the message-passing process.

TorGNN architectures: Once we get the representation vector for each node, we can use the node representation for downstream tasks. In this section, we focus on link prediction tasks and node classification tasks.

The link prediction tasks are to calculate whether or not there is an edge between two nodes or the possibility of an edge. After the message-passing process, node representations h_x and h_y are obtained for nodes x and y . The representation vector of the edge is then used as input for multilayer perceptron (MLP) to predict the possibility of the existence of the edge as follows,

$$\hat{p}(x,y) = \text{MLP}_{\text{link}}(\| (h_x + h_y, h_x \odot h_y, h_x, h_y) \|),$$

where $\| \cdot \|$ is to concatenate the vectors within the bracket into a long vector, and \odot is element-wise product. It is worth noting that various operations are used in the above equation to model the relationship between two nodes.

The node classification tasks are to predict the label of a node. In these tasks, we use the node representations learned from GNN part, and train them with a MLP model with

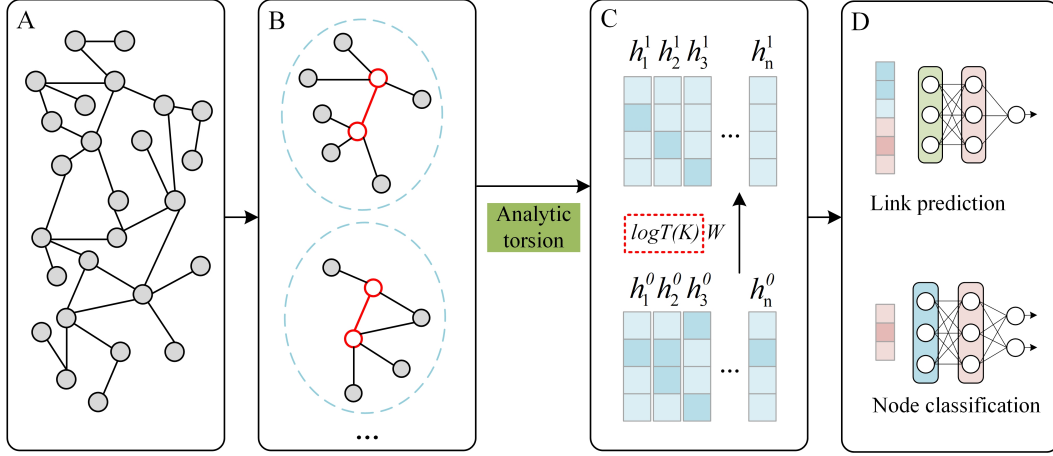


Fig. 3. **The overview of TorGNN architecture.** **A.** A large network. **B.** Local simplicial complex construction. **C.** Analytic torsion-based message-passing process. **D.** TorGNN architecture for link prediction task and node classification.

output the predicted label of the node. The process can be expressed as follows,

$$\hat{p}_x = MLP_{node}(h_x)$$

Note that in both tasks, we use the cross-entropy as loss function. A detailed illustration of our TorGNN architectures are illustrated in Figure 3. For more detailed parameter introduction of the model, please refer to the source code¹.

4 EXPERIMENTS

This section covers four tests, including a link prediction test on 16 networks, a node classification test on 3 networks, a representation learning test and a parameter analysis test. Our TorGNN model shows good performance on all tests.

4.1 Datasets

In this test, we utilize six types of datasets with a total of 19 networks to verify the performance of TorGNN. These six types of datasets include: 4 biomedical networks (HuRI-PPI [44], ChG-Miner [45], DisGeNET [46], Drugbank_DTI [47]), 4 social networks (lasftm_asia [48], twitch_EN [49], facebook_comp [50], facebook_TV [50]), 2 collaboration networks (CA-HepTh [51], CA-GrQc [51]), 3 internet peer-to-peer networks (p2p-Gnutella04 [51], p2p-Gnutella05 [51], p2p-Gnutella06 [51]), 3 autonomous systems networks (as20000102 [52], oregon1_010331 [52], oregon1_010407 [52]), and 3 citation networks (Citeseer [53], Cora [53], Pubmed [53]). Note that biomedical networks, social networks, collaboration networks, internet peer-to-peer networks and autonomous systems networks are mainly used for link prediction tasks. See Table 1 for details of these dataset. The citation networks are mainly used for node classification tasks. See Table 2 for details of the dataset.

1. A reference implementation of TorGNN may be found at <https://github.com/CS-BIO/TorGNN>

TABLE 1
Details of 16 network data on link prediction tasks.

Categories	Networks	Nodes	Edges	Density
Biomedical networks	HuRI-PPI	5604	23322	0.15%
	ChG-Miner	7341	15138	0.06%
	DisGeNET	19783	81746	0.04%
	Drugbank_DTI	12566	18866	0.02%
Social networks	lasftm_asia	7624	27806	0.10%
	twitch_EN	7126	35324	0.14%
	facebook_comp	14113	52310	0.05%
	facebook_TV	3892	17262	0.23%
Collaboration networks	CA-HepTh	9877	25998	0.05%
	CA-GrQc	5242	14496	0.11%
Internet peer-to-peer networks	p2p-Gnutella04	10876	39994	0.07%
	p2p-Gnutella05	8846	31839	0.08%
	p2p-Gnutella06	8717	31525	0.08%
Autonomous systems networks	as20000102	6474	13895	0.07%
	oregon1_010331	10670	22002	0.04%
	oregon1_010407	10729	21999	0.04%

TABLE 2
Details of 3 network data on node classification tasks.

Networks	Nodes	Edges	Density	Classes	Feature
Citeseer	3327	4732	0.09%	6	3703
Cora	2708	5429	0.15%	7	1433
Pubmed	19717	44338	0.02%	3	500

4.2 Baselines

In link prediction tasks, we compare TorGNN against state-of-the-art GNN methods and network embedding methods. We adopt a total of 5 GNN models, including LightGCN [54], SkipGNN [55], KGIN [56], GCN [2] and GAT [5]. The network embedding method is a kind of representation learning methods, and it's main goal is to reduce high-dimensional representation vectors of nodes, edges, or subgraphs into low-dimensional vectors. We select three classic network embedding methods, including DeepWalk [57], LINE [58] and SDNE [59].

In node classification tasks, we select 9 models as the comparison methods, namely ManiReg [60], SemiEmb [61], DeepWalk [57], Planetoid [53], GCN [2], DCNN [62], SAGE [3], N-GCN [9] and N-SAGE [9]. These 9 methods cover various model types that can be applied to node classification

tasks, including graph neural network, network embedding model, traditional machine model, etc. In this way, the performance of our TorGNN model can be evaluated more comprehensively.

4.3 Performance on link prediction tasks

Five types of datasets, including a total of 16 network data, are used for the evaluation of the performance of our TorGNN. For each network, we randomly sample the same number of negative and positive samples, and then divide them into training set, validation set and test set with a ratio of 7:1:2. The area under the receiver operating characteristic curve (AUC) and the area under the precision-recall curve (AUPR) are used for evaluating the performance of each model. This process is repeated 10 times, and the average value is taken as the final result. We use batch size 128 with Adam optimizer and run TorGNN model in PyTorch. For the learning rate, after adjustment, it is found that the learning rate of $5e-4$ is the most suitable for all 16 networks.

Table 3 presents the prediction results on the link prediction tasks. Overall, our TorGNN model outperforms other models on most datasets, and the average AUC and AUPR on 16 networks are 2.49% and 3.45% higher than the second-ranked model, respectively. It is worth noting that the performance of the TorGNN model on all data sets is better than that of the 3 network embedding models (DeepWalk, LINE and SDNE), which shows that the TorGNN model is not only a good graph neural network model, but also an excellent network embedding models. Although the AUC value of the TorGNN model on the “as20000102” network and the AUPR value on the “facebook_comp” network did not reach the highest value, the AUPR value of the TorGNN model on the “as20000102” network and the AUC value on the “facebook_comp” network are still the best. Note that our tasks are from various types of networks, including biomedical networks, collaboration networks and internet peer-to-peer networks, the great performance of our TorGNN shows that it has a strong generalization capability for network/graph data.

4.4 Performance on node classification tasks.

Three networks, including Citeseer, Cora and Pubmed, are used in the evaluation of the performance of TorGNN model. Following the general way to set up training, verification and test sets of these three datasets [63], we select 500 nodes in each data set as the verification set, 1000 nodes as the test set, and the remaining nodes as the training set. The accuracy is used to evaluate the performance of TorGNN. Each step is run 10 times, and the average is taken as the final result. We use Adam optimizer of learning rate 0.02 and run TorGNN model in PyTorch.

Figure 4 shows the results of the TorGNN model and the comparison methods for node classification tasks on three datasets. Our TorGNN model has achieved the best results, and it is significantly better than the second-ranked model N-GCN. It is worth noting that N-GCN and N-SAGE are improved models based on GCN and SAGE. Specifically, they use a data perturbation method to prevent overfitting of the traditional model. As can be seen in Figure 4, the performance of N-GCN and N-SAGE models is superior

to the traditional GCN and SAGE models. Nevertheless, these models are still slightly inferior to our TorGNN model, which shows that the advantages of our TorGNN model over the traditional GNNs are not only reflected in the overall performance, but also in preventing overfitting. The reason may be that the analytic torsion of the local structure plays a restrictive role in the adjustment of the parameters in GNNs and reduces overfitting.

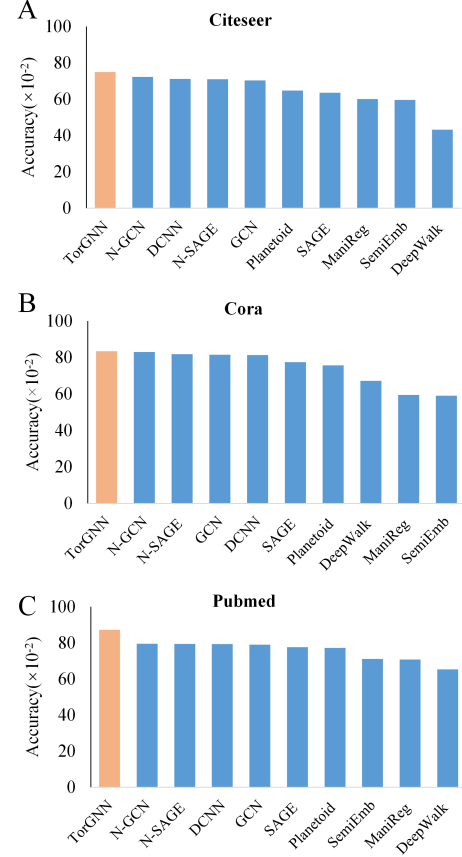


Fig. 4. The comparison of different models on node classification performance based on three citation datasets. A, B, and C illustrate the comparison of accuracy for various models on Citeseer, Cora and Pubmed datasets, respectively.

4.5 Performance on representation learning

To further illustrate the representation learning ability of our TorGNN, we set up a visualization test. First, we get the representation vectors for node pairs in the test sets. Then, we use t-SNE [64] to project the high-dimensional representation vectors to 2D space, where the representation vectors are mainly divided into two categories, positive samples (node pairs with link relationship) and negative samples (node pairs without link relationship). Finally, these representation vectors in 2D space are illustrated in Figure 5 (red and blue points represent negative and positive samples, respectively). Three datasets of HuRI-PPI, ChG-Miner and Drugbank_DTI are used in our test. At the same time, we choose DeepWalk, LINE and SDNE three network embedding methods for comparison. It can be seen from Figure 5 that our TorGNN model has obvious advantages in distinguishing node pairs

TABLE 3
The comparison of different models on link prediction based on 16 datasets. The measurements are AUC and AUPR.

	Networks	TorGNN	LightGCN	SkipGNN	KGIN	GCN	GAT	DeepWalk	LINE	SDNE
AUC	HuRI-PPI	0.9369	0.8170	0.9119	0.9007	0.9164	0.8994	0.7294	0.8223	0.9243
	ChG-Miner	0.9583	0.7457	0.9526	0.9493	0.9352	0.9514	0.8093	0.7036	0.6108
	DisGeNET	0.9868	0.8597	0.9145	0.9154	0.9723	0.9829	0.6922	0.8492	0.9586
	Drugbank_DTI	0.9651	0.6821	0.8946	0.9453	0.9234	0.9476	0.8572	0.6312	0.8522
	lasftm_asia	0.9204	0.8787	0.8117	0.9125	0.8693	0.8619	0.7312	0.8049	0.8952
	twitch_EN	0.9159	0.8071	0.8640	0.8807	0.8965	0.8863	0.6823	0.7836	0.8627
	facebook_comp	0.8974	0.8793	0.7823	0.9146	0.8614	0.8598	0.7525	0.6756	0.7733
	facebook_TV	0.9500	0.9164	0.7941	0.8951	0.9146	0.9165	0.8637	0.6841	0.8145
	CA-HepTh	0.9476	0.6004	0.7859	0.8117	0.9206	0.9185	0.7454	0.6285	0.8514
	CA-GrQc	0.9599	0.8304	0.8062	0.8084	0.9430	0.9420	0.8224	0.7307	0.8785
	p2p-Gnutella04	0.9060	0.6232	0.8034	0.8898	0.8901	0.8816	0.6175	0.5980	0.7883
	p2p-Gnutella05	0.8956	0.6037	0.8074	0.8871	0.8847	0.8785	0.6353	0.5945	0.8051
	p2p-Gnutella06	0.9051	0.6240	0.8112	0.8864	0.8872	0.8828	0.6490	0.5687	0.8003
	as20000102	0.9292	0.7834	0.9125	0.9334	0.9120	0.8926	0.8276	0.8340	0.8902
	oregon1_010331	0.9602	0.7913	0.9544	0.9450	0.9516	0.9338	0.8165	0.8812	0.9219
	oregon1_010407	0.9603	0.8060	0.9492	0.9416	0.9518	0.9594	0.8142	0.8657	0.9172
	Average	0.9372	0.7655	0.8597	0.9011	0.9144	0.9107	0.7529	0.7285	0.8465
AUPR	HuRI-PPI	0.9424	0.8589	0.9182	0.9006	0.9189	0.8965	0.6958	0.8520	0.9324
	ChG-Miner	0.9606	0.8006	0.9524	0.9493	0.9409	0.9499	0.8267	0.7514	0.6114
	DisGeNET	0.9882	0.8915	0.9271	0.9154	0.9785	0.9849	0.6846	0.8477	0.9554
	Drugbank_DTI	0.9664	0.7593	0.6764	0.9452	0.9371	0.9533	0.8729	0.7044	0.8672
	lasftm_asia	0.9311	0.9028	0.8269	0.9124	0.8810	0.8810	0.7365	0.8395	0.9127
	twitch_EN	0.9265	0.8573	0.8750	0.8807	0.9051	0.8899	0.6729	0.8134	0.8642
	facebook_comp	0.9112	0.9045	0.7993	0.9146	0.8761	0.871	0.7517	0.6956	0.8092
	facebook_TV	0.9569	0.9359	0.8116	0.8951	0.9256	0.9265	0.8672	0.7461	0.8517
	CA-HepTh	0.9487	0.5991	0.7889	0.7794	0.9169	0.9077	0.7313	0.6778	0.8614
	CA-GrQc	0.9626	0.8275	0.8228	0.7769	0.9427	0.9419	0.8469	0.7863	0.8845
	p2p-Gnutella04	0.9027	0.6884	0.7660	0.8898	0.8901	0.8843	0.6166	0.5967	0.7735
	p2p-Gnutella05	0.8892	0.6764	0.7748	0.8870	0.8804	0.8751	0.6514	0.6177	0.7838
	p2p-Gnutella06	0.8996	0.6918	0.7763	0.8862	0.8830	0.8814	0.6457	0.5976	0.7718
	as20000102	0.9383	0.8403	0.9333	0.9334	0.9290	0.9090	0.8157	0.8742	0.9159
	oregon1_010331	0.9638	0.8397	0.9601	0.9450	0.9596	0.9448	0.8088	0.9042	0.9354
	oregon1_010407	0.9649	0.8573	0.9604	0.9415	0.9596	0.9448	0.7888	0.8987	0.9335
	Average	0.9319	0.9008	0.8355	0.8685	0.8649	0.8477	0.7731	0.7575	0.7992

with and without link relationship, which shows that our TorGNN model has a better ability in representation learning than traditional network embedding model.

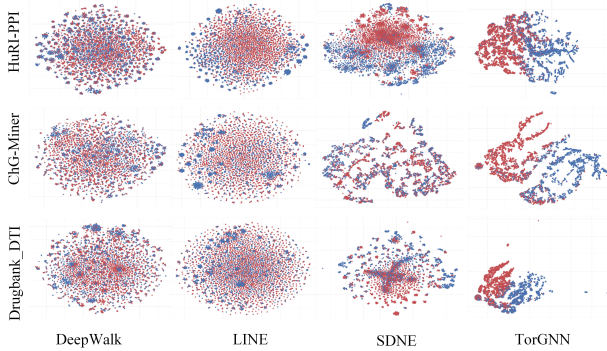


Fig. 5. The comparison of the representation learning capability of different models on HuRI-PPI, ChG-Miner and Drugbank_DTI network datasets. The representation vectors of each nodes in the test datasets are projected into 2D spaces by t-SNE. The red and blue points represent node pairs without and with link relationships, respectively. Four network embedding methods are considered in our comparison.

4.6 Influence of local simplicial complex

In order to analyze the impact of the number of neighbor layers and the highest order of the local simplicial complex on $\text{TorGNN}(l_{\text{sub}}, n)$, we set up the following parameter analysis model:

- $\text{TorGNN}(1,1)$: $l_{\text{sub}}=1, n=1$. It means that TorGNN only considers first-order neighbors when constructed local simplicial complex, the highest order of the simplicial complex is only up to 1, that is, only edges are considered.
- $\text{TorGNN}(1,2)$: $l_{\text{sub}}=1, n=2$. It means that TorGNN only considers first-order neighbors when constructed local simplicial complex, the highest order of the simplicial complex is up to 2, that is, triangles (2-simplices) are considered.
- $\text{TorGNN}(2,1)$: $l_{\text{sub}}=2, n=1$. It means that TorGNN considers second-order neighbors when constructed local simplicial complex, the highest order of the simplicial complex is only up to 1, that is, only edges are considered.

Table 4 and Table 5 show the results of these three models on link prediction tasks and node classification tasks. It can be seen that the performance of the three models are relatively stable. The differences between the three models for both AUC and AUPR are less than 0.02 for all the test cases, except “drugbank_DTI”, “facebook_comp” and “p2p-Gnutella06”. Comparably speaking, $\text{TorGNN}(2,1)$ model has the best overall performance. This may due to the reason that the corresponding local simplicial complex of $\text{TorGNN}(2,1)$ has a better representability of the local structures. Note that with $l_{\text{sub}} = 2$, the local simplicial complex contains all second-order neighbors and is a much larger structure. Computationally, more efficient algorithms will be needed

for the fast evaluation of the analytical torsion if large-sized simplicial complex is used.

TABLE 4
Effect of parameters on link prediction tasks of TorGNN(l_{sub}, n).

Networks	TorGNN(1,1)		TorGNN(1,2)		TorGNN(2,1)	
	AUC	AUPR	AUC	AUPR	AUC	AUPR
HuRI-PPI	0.9369	0.9424	0.9308	0.9377	0.9357	0.9370
ChG-Miner	0.9533	0.9570	0.9475	0.9524	0.9583	0.9606
DisGeNET	0.9868	0.9882	0.9840	0.9857	NA ¹	NA ¹
drugbank_DTI	0.9380	0.9469	0.9306	0.9411	0.9651	0.9664
lasftm_asia	0.9152	0.9261	0.8997	0.9150	0.9204	0.9311
twitch_EN	0.9159	0.9265	0.9066	0.9168	NA ¹	NA ¹
facebook_comp	0.8974	0.9112	0.8865	0.9012	0.8573	0.8682
facebook_TV	0.9488	0.9564	NA ¹	NA ¹	0.9500	0.9569
CA-HepTh	0.9427	0.9430	0.9289	0.9288	0.9476	0.9487
CA-GrQc	0.9573	0.9597	0.9328	0.9373	0.9599	0.9626
p2p-Gnutella04	0.9024	0.9026	0.8898	0.8923	0.9060	0.9027
p2p-Gnutella05	0.8883	0.8858	0.8843	0.8836	0.8956	0.8892
p2p-Gnutella06	0.8464	0.8978	0.8913	0.8908	0.9051	0.8996
as20000102	0.9274	0.9364	0.9216	0.9335	0.9292	0.9383
oregon1_010331	0.9590	0.9642	0.9505	0.9593	0.9602	0.9638
oregon1_010407	0.9603	0.9649	0.9524	0.9600	0.9590	0.9637

¹ NA indicates that the model requires too much memory or time.

TABLE 5
Effect of parameters on node classification tasks of TorGNN(l_{sub}, n).

Networks	Accuracy		
	TorGNN(1,1)	TorGNN(1,2)	TorGNN(2,1)
Citeseer	0.748	0.746	0.749
Cora	0.832	0.823	0.834
Pubmed	0.865	0.872	0.868

5 CONCLUSION

The incorporation of geometric and topological information into graph neural architecture remains to be a key issue for geometric deep learning models, in particular graph neural network models.

In this paper, we propose an analytic torsion enhanced graph neural network (TorGNN) model, which mainly uses analytic torsion to capture the complexity of the structures, and then incorporate it into message-passing process to improve the performance of the traditional graph neural network models. From the tasks of link prediction and node classification, our TorGNN is found to be not only better than traditional GNNs models, but also better than other graph deep learning models.

ACKNOWLEDGEMENTS

This work was supported in part by National Natural Science Foundation of China (NSFC grant no. 61873089, 62032007), Nanyang Technological University Startup Grant (grant no. M4081842), Singapore Ministry of Education Academic Research fund (grant no. Tier 1 RG109/19, MOE-T2EP20120-0013, MOE-T2EP20220-0010) and China Scholarship Council (CSC grant no.202006130147).

REFERENCES

[1] Y. LeCun, Y. Bengio, and G. Hinton, "Deep learning," *nature*, vol. 521, no. 7553, pp. 436–444, 2015.

[2] M. Welling and T. N. Kipf, "Semi-supervised classification with graph convolutional networks," in *J. International Conference on Learning Representations (ICLR 2017)*, 2016.

[3] W. Hamilton, Z. Ying, and J. Leskovec, "Inductive representation learning on large graphs," *Advances in neural information processing systems*, vol. 30, 2017.

[4] S. Vashishth, S. Sanyal, V. Nitin, and P. Talukdar, "Composition-based multi-relational graph convolutional networks," *arXiv preprint arXiv:1911.03082*, 2019.

[5] P. Veličković, G. Cucurull, A. Casanova, A. Romero, P. Lio, and Y. Bengio, "Graph attention networks," *arXiv preprint arXiv:1710.10903*, 2017.

[6] A. Fout, J. Byrd, B. Shariat, and A. Ben-Hur, "Protein interface prediction using graph convolutional networks," *Advances in neural information processing systems*, vol. 30, 2017.

[7] W. Fan, Y. Ma, Q. Li, Y. He, E. Zhao, J. Tang, and D. Yin, "Graph neural networks for social recommendation," in *The world wide web conference*, 2019, pp. 417–426.

[8] T. Young, D. Hazarika, S. Poria, and E. Cambria, "Recent trends in deep learning based natural language processing," *IEEE Computational intelligence magazine*, vol. 13, no. 3, pp. 55–75, 2018.

[9] S. Abu-El-Haija, A. Kapoor, B. Perozzi, and J. Lee, "N-GCN: Multi-scale graph convolution for semi-supervised node classification," in *Uncertainty in artificial intelligence*. PMLR, 2020, pp. 841–851.

[10] Y. Shen, J. Qin, J. Chen, M. Yu, L. Liu, F. Zhu, F. Shen, and L. Shao, "Auto-encoding twin-bottleneck hashing," in *Proceedings of the IEEE/CVF Conference on Computer Vision and Pattern Recognition*, 2020, pp. 2818–2827.

[11] X. Ju, S. Farrell, P. Calafiura, D. Murnane, L. Gray, T. Klijsma, K. Pedro, G. Cerati, J. Kowalkowski, G. Perdue *et al.*, "Graph neural networks for particle reconstruction in high energy physics detectors," *arXiv preprint arXiv:2003.11603*, 2020.

[12] K. Rusek and P. Cholda, "Message-passing neural networks learn little's law," *IEEE Communications Letters*, vol. 23, no. 2, pp. 274–277, 2018.

[13] S. Abadal, A. Jain, R. Guirado, J. López-Alonso, and E. Alarcón, "Computing graph neural networks: A survey from algorithms to accelerators," *ACM Computing Surveys (CSUR)*, vol. 54, no. 9, pp. 1–38, 2021.

[14] J. Zhou, G. Cui, S. Hu, Z. Zhang, C. Yang, Z. Liu, L. Wang, C. Li, and M. Sun, "Graph neural networks: A review of methods and applications," *AI Open*, vol. 1, pp. 57–81, 2020.

[15] S. Sukhbaatar, R. Fergus *et al.*, "Learning multiagent communication with backpropagation," *Advances in neural information processing systems*, vol. 29, 2016.

[16] Y. Li, D. Tarlow, M. Brockschmidt, and R. Zemel, "Gated graph sequence neural networks," *arXiv preprint arXiv:1511.05493*, 2015.

[17] Z. Ye, K. S. Liu, T. Ma, J. Gao, and C. Chen, "Curvature graph network," in *International Conference on Learning Representations*, 2019.

[18] J. Chen, T. Ma, and C. Xiao, "FastGCN: fast learning with graph convolutional networks via importance sampling," *arXiv preprint arXiv:1801.10247*, 2018.

[19] W.-L. Chiang, X. Liu, S. Si, Y. Li, S. Bengio, and C.-J. Hsieh, "ClusterGCN: An efficient algorithm for training deep and large graph convolutional networks," in *Proceedings of the 25th ACM SIGKDD international conference on knowledge discovery & data mining*, 2019, pp. 257–266.

[20] H. Gao, Z. Wang, and S. Ji, "Large-scale learnable graph convolutional networks," in *Proceedings of the 24th ACM SIGKDD international conference on knowledge discovery & data mining*, 2018, pp. 1416–1424.

[21] S. Yan, Y. Xiong, and D. Lin, "Spatial temporal graph convolutional networks for skeleton-based action recognition," in *Thirty-second AAAI conference on artificial intelligence*, 2018.

[22] R. Li, S. Wang, F. Zhu, and J. Huang, "Adaptive graph convolutional neural networks," in *Proceedings of the AAAI conference on artificial intelligence*, vol. 32, no. 1, 2018.

[23] F. Wu, A. Souza, T. Zhang, C. Fifty, T. Yu, and K. Weinberger, "Simplifying graph convolutional networks," in *International conference on machine learning*. PMLR, 2019, pp. 6861–6871.

[24] W. Yu, C. Zheng, W. Cheng, C. C. Aggarwal, D. Song, B. Zong, H. Chen, and W. Wang, "Learning deep network representations with adversarially regularized autoencoders," in *Proceedings of the 24th ACM SIGKDD international conference on knowledge discovery & data mining*, 2018, pp. 2663–2671.

- [25] N. De Cao and T. Kipf, “MolGAN: An implicit generative model for small molecular graphs,” *arXiv preprint arXiv:1805.11973*, 2018.
- [26] R. Das, S. Dhuliawala, M. Zaheer, L. Vilnis, I. Durugkar, A. Krishnamurthy, A. Smola, and A. McCallum, “Go for a walk and arrive at the answer: Reasoning over paths in knowledge bases using reinforcement learning,” *arXiv preprint arXiv:1711.05851*, 2017.
- [27] J. Topping, F. Di Giovanni, B. P. Chamberlain, X. Dong, and M. M. Bronstein, “Understanding over-squashing and bottlenecks on graphs via curvature,” *International Conference on Learning Representations (ICLR 2022)*, 2021.
- [28] J. Li, X. Fu, Q. Sun, C. Ji, J. Tan, J. Wu, and H. Peng, “Curvature graph generative adversarial networks,” in *Proceedings of the ACM Web Conference 2022*, 2022, pp. 1528–1537.
- [29] V. Turaev, *Introduction to combinatorial torsions*. Springer Science & Business Media, 2001.
- [30] A. Grigor’yan, Y. Lin, and S.-T. Yau, “Torsion of digraphs and path complexes,” *arXiv preprint arXiv:2012.07302*, 2020.
- [31] D. B. Ray and I. M. Singer, “R-torsion and the laplacian on riemannian manifolds,” *Advances in Mathematics*, vol. 7, no. 2, pp. 145–210, 1971.
- [32] K. Reidemeister, “Homotopieringe und linsenräume,” in *Abhandlungen aus dem Mathematischen Seminar der Universität Hamburg*, vol. 11, no. 1. Springer, 1935, pp. 102–109.
- [33] W. Müller, “Analytic torsion and R-torsion of riemannian manifolds,” *Advances in Mathematics*, vol. 28, no. 3, pp. 233–305, 1978.
- [34] J. Cheeger, “Analytic torsion and Reidemeister torsion,” *Proceedings of the National Academy of Sciences*, vol. 74, no. 7, pp. 2651–2654, 1977.
- [35] N. Thomas, T. Smidt, S. Kearnes, L. Yang, L. Li, K. Kohlhoff, and P. Riley, “Tensor field networks: Rotation-and translation-equivariant neural networks for 3D point clouds,” *arXiv preprint arXiv:1802.08219*, 2018.
- [36] M. Finzi, S. Stanton, P. Izmailov, and A. G. Wilson, “Generalizing convolutional neural networks for equivariance to lie groups on arbitrary continuous data,” in *International Conference on Machine Learning*. PMLR, 2020, pp. 3165–3176.
- [37] V. G. Satorras, E. Hoogeboom, and M. Welling, “E(n) equivariant graph neural networks,” in *International conference on machine learning*. PMLR, 2021, pp. 9323–9332.
- [38] L. Sun, Z. Zhang, J. Ye, H. Peng, J. Zhang, S. Su, and S. Y. Philip, “A self-supervised mixed-curvature graph neural network,” in *Proceedings of the AAAI Conference on Artificial Intelligence*, vol. 36, no. 4, 2022, pp. 4146–4155.
- [39] I. Chami, Z. Ying, C. Ré, and J. Leskovec, “Hyperbolic graph convolutional neural networks,” *Advances in neural information processing systems*, vol. 32, 2019.
- [40] Y. Zhang, X. Wang, C. Shi, X. Jiang, and Y. Ye, “Hyperbolic graph attention network,” *IEEE Transactions on Big Data*, vol. 8, no. 6, pp. 1690–1701, 2021.
- [41] Q. Liu, M. Nickel, and D. Kiela, “Hyperbolic graph neural networks,” *Advances in Neural Information Processing Systems*, vol. 32, 2019.
- [42] X. Fu, J. Li, J. Wu, Q. Sun, C. Ji, S. Wang, J. Tan, H. Peng, and S. Y. Philip, “ACE-HGNN: Adaptive curvature exploration hyperbolic graph neural network,” in *2021 IEEE International Conference on Data Mining (ICDM)*. IEEE, 2021, pp. 111–120.
- [43] Z. Wu, D. Jiang, C.-Y. Hsieh, G. Chen, B. Liao, D. Cao, and T. Hou, “Hyperbolic relational graph convolution networks plus: a simple but highly efficient QSAR-modeling method,” *Briefings in Bioinformatics*, vol. 22, no. 5, p. bbab112, 2021.
- [44] K. Luck, D.-K. Kim, L. Lambourne, K. Spirohn, B. E. Begg, W. Bian, R. Brignall, T. Cafarelli, F. J. Campos-Laborie, B. Charlotiaux *et al.*, “A reference map of the human binary protein interactome,” *Nature*, vol. 580, no. 7803, pp. 402–408, 2020.
- [45] Z. Marinka, S. Rok, M. Sagar, , and L. Jure, “BioSNAP Datasets: Stanford biomedical network dataset collection,” <http://snap.stanford.edu/biodata>, Aug. 2018.
- [46] J. Piñero, À. Bravo, N. Queralt-Rosinach, A. Gutiérrez-Sacristán, J. Deu-Pons, E. Centeno, J. García-García, F. Sanz, and L. I. Furlong, “DisGeNET: a comprehensive platform integrating information on human disease-associated genes and variants,” *Nucleic acids research*, p. gkw943, 2016.
- [47] D. S. Wishart, Y. D. Feunang, A. C. Guo, E. J. Lo, A. Marcu, J. R. Grant, T. Sajed, D. Johnson, C. Li, Z. Sayeeda *et al.*, “DrugBank 5.0: a major update to the drugbank database for 2018,” *Nucleic acids research*, vol. 46, no. D1, pp. D1074–D1082, 2018.
- [48] B. Rozemberczki and R. Sarkar, “Characteristic functions on graphs: Birds of a feather, from statistical descriptors to parametric models,” in *Proceedings of the 29th ACM international conference on information & knowledge management*, 2020, pp. 1325–1334.
- [49] B. Rozemberczki, C. Allen, and R. Sarkar, “Multi-scale attributed node embedding,” 2019.
- [50] B. Rozemberczki, R. Davies, R. Sarkar, and C. Sutton, “GEMSEC: Graph embedding with self clustering,” in *Proceedings of the 2019 IEEE/ACM International Conference on Advances in Social Networks Analysis and Mining 2019*. ACM, 2019, pp. 65–72.
- [51] J. Leskovec, J. Kleinberg, and C. Faloutsos, “Graph evolution: Densification and shrinking diameters,” *ACM transactions on Knowledge Discovery from Data (TKDD)*, vol. 1, no. 1, pp. 2–es, 2007.
- [52] —, “Graphs over time: densification laws, shrinking diameters and possible explanations,” in *Proceedings of the eleventh ACM SIGKDD international conference on Knowledge discovery in data mining*, 2005, pp. 177–187.
- [53] Z. Yang, W. Cohen, and R. Salakhudinov, “Revisiting semi-supervised learning with graph embeddings,” in *International conference on machine learning*. PMLR, 2016, pp. 40–48.
- [54] X. He, K. Deng, X. Wang, Y. Li, Y. Zhang, and M. Wang, “LightGCN: Simplifying and powering graph convolution network for recommendation,” in *Proceedings of the 43rd International ACM SIGIR conference on research and development in Information Retrieval*, 2020, pp. 639–648.
- [55] K. Huang, C. Xiao, L. M. Glass, M. Zitnik, and J. Sun, “SkipGNN: predicting molecular interactions with skip-graph networks,” *Scientific reports*, vol. 10, no. 1, pp. 1–16, 2020.
- [56] X. Wang, T. Huang, D. Wang, Y. Yuan, Z. Liu, X. He, and T.-S. Chua, “Learning intents behind interactions with knowledge graph for recommendation,” in *Proceedings of the Web Conference 2021*, 2021, pp. 878–887.
- [57] B. Perozzi, R. Al-Rfou, and S. Skiena, “DeepWalk: Online learning of social representations,” in *Proceedings of the 20th ACM SIGKDD international conference on Knowledge discovery and data mining*, 2014, pp. 701–710.
- [58] J. Tang, M. Qu, M. Wang, M. Zhang, J. Yan, and Q. Mei, “Line: Large-scale information network embedding,” in *Proceedings of the 24th international conference on world wide web*, 2015, pp. 1067–1077.
- [59] D. Wang, P. Cui, and W. Zhu, “Structural deep network embedding,” in *Proceedings of the 22nd ACM SIGKDD international conference on Knowledge discovery and data mining*, 2016, pp. 1225–1234.
- [60] M. Belkin, P. Niyogi, and V. Sindhwani, “Manifold regularization: A geometric framework for learning from labeled and unlabeled examples,” *Journal of machine learning research*, vol. 7, no. 11, 2006.
- [61] J. Weston, F. Ratle, and R. Collobert, “Deep learning via semi-supervised embedding,” in *Proceedings of the 25th international conference on Machine learning*, 2008, pp. 1168–1175.
- [62] J. Atwood and D. Towsley, “Diffusion-convolutional neural networks,” *Advances in neural information processing systems*, vol. 29, 2016.
- [63] Y. Rong, W. Huang, T. Xu, and J. Huang, “Dropedge: Towards deep graph convolutional networks on node classification,” *arXiv preprint arXiv:1907.10903*, 2019.
- [64] L. Van der Maaten and G. Hinton, “Visualizing data using t-SNE,” *Journal of machine learning research*, vol. 9, no. 11, 2008.